ISSN 1063-7826, Semiconductors, 2009, Vol. 43, No. 12, pp. 1610–1616. © Pleiades Publishing, Ltd., 2009.
Original Russian Text © P.V. Seredin, A.V. Glotov, E.P. Domashevskaya, I.N. Arsentyev, D.A. Vinokurov, A.L. Stankevich, I.S. Tarasov, 2009, published in Fizika i Tekhnika Poluprovodnikov, 2009, Vol. 43, No. 12, pp. 1654–1661.

FABRICATION, TREATMENT, AND TESTING OF MATERIALS AND STRUCTURES

Structural and Optical Properties of Low-Temperature Hydride-MOCVD AlGaAs/GaAs(100) Heterostructures Based on Omission Solid Solutions

P. V. Seredin[a]^, A. V. Glotov[a], E. P. Domashevskaya[a], I. N. Arsentyev[b]^^, D. A. Vinokurov[b], A. L. Stankevich[b], and I. S. Tarasov[b]

[a] *Voronezh State University, Universitetskaya pl. 1, Voronezh, 394006 Russia*
^e-mail: Paul@phys.vsu.ru,
[b] *Ioffe Physicotechnical Institute, Russian Academy of Sciences, ul. Polytekhnicheskaya 26, St.Petersburg, 194021 Russia*
^^e-mail: Arsentyev@mail.ioffe.ru

Submitted April 29, 2009; accepted for publication April 30, 2009

Abstract—X-ray diffraction, scanning electron microscopy, and IR reflectance spectroscopy were used to study properties of epitaxial low-temperature hydride-MOCVD AlGaAs/GaAs (100) heterostructures. It was found that the variation in the AlGaAs alloy lattice's parameter with Al content does not obey the classical Vegard's law, and the lattice parameters are smaller than those of GaAs.

PACS numbers: 64.70.N..., 68.37.-d, 68.55.-a

DOI: 10.1134/S1063782609120070

1. INTRODUCTION

Epitaxial AlGaAs alloys grown on GaAs substrates represent the most lattice-constant-matched heterostructure and gained wide acceptance and is one of the most used components of electronic and optoelectronic engineering. The AlAs–GaAs system has long been studied; currently, all main properties of its semiconductor alloys have been comprehensively studied, and their various dependences are reference values. However, as has been repeatedly shown, the effect of various factors such as nonequilibrium thermodynamic processes in reactors, strain fields caused by the slightest mismatches of the film and substrate's lattice parameters [1–3], makes it possible to achieve radically new properties of heterostructures even in such a well studied system.

For example, as was shown in some studies, an $AlGaAs_2$ superstructure phase can be formed in $Al_xGa_{1-x}As$/GaAs (100) heterostructures at $x \approx 0.50$. The lattice of such an ordering phase can be described by the $InGaAs_2$-type (layered tetragonal) structure [4] with the [100] ordering direction. In this structure, the unit cell corresponds to two sphalerite-type cells standing upon another along the **c** axis. The ratio **c** : 2**a** observed in the $AlGaAs_2$ phase was less than unity, ~0.997, which does not contradict the published data [5].

The decrease in the lattice parameter of the detected $AlGaAs_2$ superstructure was explained by the fact that Al and Ga atoms in an ideal AlGaAs solid solution are statistically distributed in the metal sublattice; hence, the lattice parameter is an average value for many cells. In the case of the superstructure, the $AlGaAs_2$ chemical compound is formed. As a result, the so-called tetragonal compression occurs due to layer ordering of the Al and Ga atomic arrangement in the Group-III sublattice, and the $AlGaAs_2$ phase parameter $\mathbf{c} < 2\mathbf{a}_{Al_{0.50}Ga_{0.50}As}$. In this case, the parameter **c** is directed perpendicularly to the (100) plane, i.e., tetragonal compression of the unit cell occurred in the direction of epitaxial film growth.

As for Vegard's law, the published papers on solid solutions in the AlAs–GaAs system show ambiguous data on its behavior (linear or nonlinear) [6, 7]. In this case, it is important to note that the dependence of the lattice parameter on the concentration of atoms in unordered homomorphic AlGaAs solid solutions, including those in which ordering was detected, obeyed the linear Vegard's law [2], and the lattice parameter increased with Al content in comparison with that of the GaAs single-crystal substrate. At the same time, the parameter of the $AlGaAs_2$ superstructure phase was smaller than the GaAs parameter, and this phase did not satisfy the existing Vegard's law [2, 3].

Moreover, the formation of the superstructure phase appears in complication of the IR reflectance spectra, and the formation of an ordered nanoprofile on the heterostructure surface with a structuring step multiple of the lattice parameter of the $AlGaAs_2$ superstructure phase.

Thus, production of new chemical compounds in the AlAs–GaAs system is of doubtless interest, and properties of such compounds deserve careful study by various methods, since modification of fundamental properties, caused by symmetry reduction of the sphalerite structure of III–V compounds, should cause a change in the band gap, possible indirect-to-direct-gap transition, inverse sequence of bands, and complication of optical spectra due to state degeneracy removal.

2. OBJECTS AND METHODS OF STUDY

The tested samples, i.e., AlGaAs/GaAs (100) heterostructures, were grown to study self-doping processes to achieve a maximum concentration of carbon acceptor. To this end, experiments were performed at a lower temperature and a minimum (3–5) ratio of Group-V and -III elements depending on the specified alloy composition.

Samples EM1540, EM1555, and EM1585 were grown using an EMCORE GS 3/100 hydride-MOCVD setup in a vertical reactor with a high rotation rate of the substrate holder. The substrate holder's temperature was 550°C, the reactor pressure was 77 Torr, and the substrate holder's rotation rate was 1000 rpm. As initial reagents, gallium trimethyl $Ga(CH_3)_3$, aluminum trimethyl $Al(CH_3)_3$, and arsine AsH_3 were used. The thickness and composition of grown layers were calculated from the data determined for layers grown under "normal conditions" (the growth temperature is 700–800°C and the ratio of Group-V and -III elements is ~100–200). To compare the properties of the samples grown by the new technique and under normal conditions, sample EM1017 grown by conventional technology was used.

Expected sample compositions and thicknesses are listed in Table 1. The structural quality and lattice parameters of alloy samples were determined by X-ray diffraction using an ARL X'TRA Thermo Techno diffractometer with high angular resolution using $Cu_{K_{\alpha 1,2}}$ radiation. IR reflectance spectra of heterostructures were measured using a Vertex-70 Bruker IR Fourier spectrometer. The surface morphology was studied using a JOEL scanning electron microscope, and element concentrations in the alloy were refined by X-ray microanalysis using an Oxford Instruments attachment.

3. RESULTS AND DISCUSSION

3.1. X-Ray Diffraction Study

Figure 1 shows the survey X-ray diffraction pattern of the AlGaAs/GaAs (100) epitaxial heterostructure (sample EM1585) in the angular range 2θ = 20°–120°. We can see that there are reflections which can be observed due to the [100] heterostructure's growth orientation, i.e., diffraction from (200), (400), and (600) planes. No additional reflections were observed, which indicates the formation of the alloy with a cubic sphalerite structure.

Table 1. Composition and layer thicknesses of AlGaAs/GaAs (100) heterostructures

Sample	x	d, μm
EM1017	0.50	~1.0
EM1540	0.00	~1.2
EM1555	0.60	~2.0
EM1585	0.40	~1.5

Accurate determination of the alloy lattice's parameter plays an important role, especially in further calculations of such values as internal strains. Minimizing the instrumental error in the diffraction angle's determination (using high-resolution diffractometers), the highest accuracy in the parameter determination can be achieved using the last (far) diffraction lines. Therefore, the study of the composition and structural quality of the heterostructures under study was performed by (600) diffraction line profiles in the angular range of 109°–111°. The accuracy of the determination of interplane distances and lattice parameters was ~0.0001 Å.

The lattice constant $\mathbf{a}^v$ of alloys, taking into account elastic strains in the heteroepitaxial layer, according to the linear elasticity theory, can be calculated as [3]

$$a^v = a^{\perp}\frac{I-v}{1+v} + a^{\parallel}\frac{2v}{1+v}, \quad (1)$$

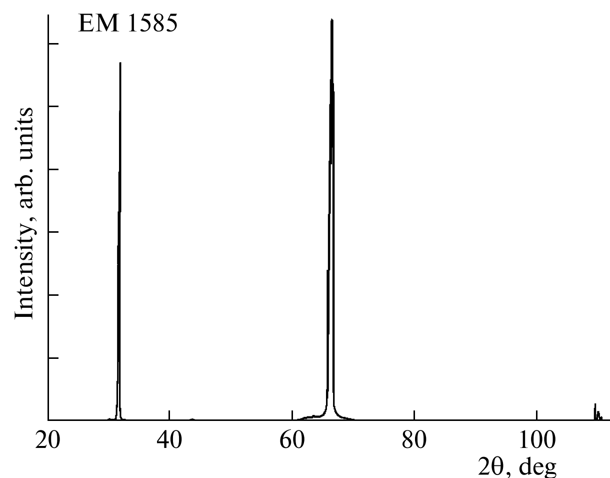

Fig. 1. Survey's X-ray diffraction pattern of autoepitaxial sample EM1585.

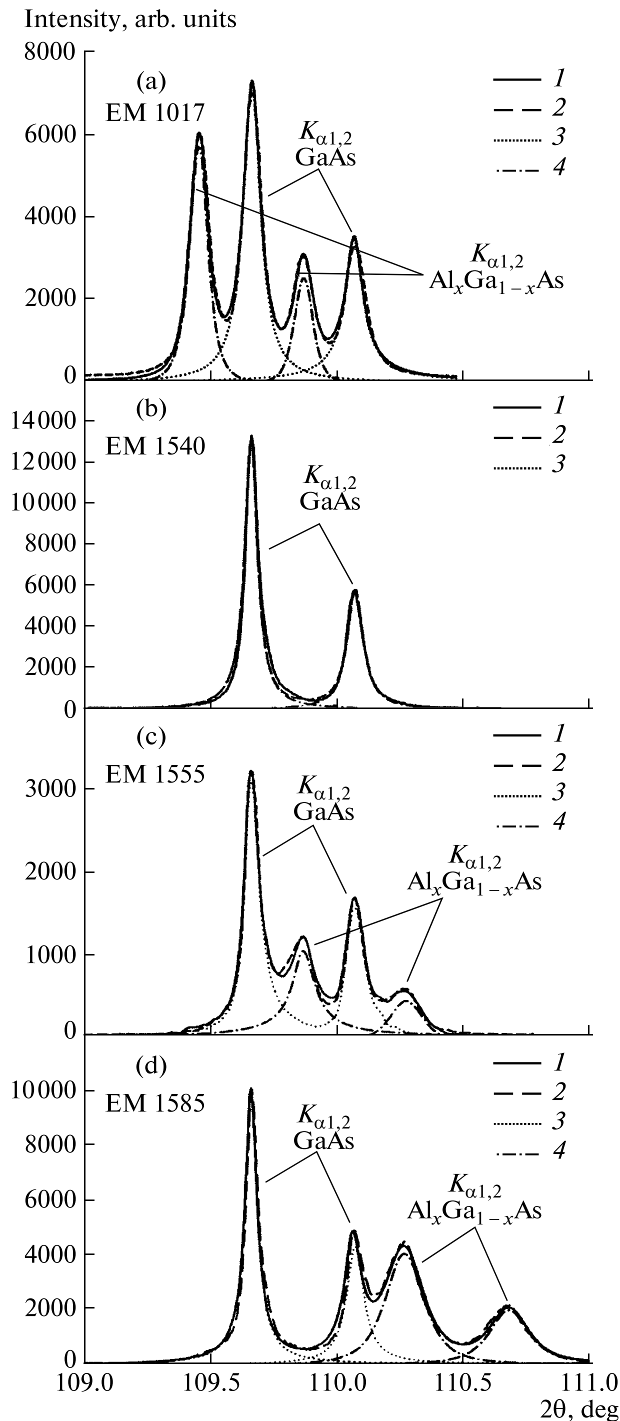

Fig. 2. Profiles of X-ray diffraction from the (600) plane for the studied heterostructure samples (a) EM1017, (b) EM1540, (c) EM1555, and (d) EM1585: (*1*) experiment, (*2*) model, (*3*) GaAs (100) substrate, and (*4*) AlGaAs alloy.

where v are the Poisson ratios for epitaxial layers, $a^{\perp}$ and $a^{\parallel}$ are the perpendicular and parallel components of the lattice parameter. Thus, the expressions for the lattice parameter of AlGaAs epitaxial layers are given by

$$a_{Al_xGa_{1-x}As} = a^{\perp}_{Al_xGa_{1-x}As}\frac{1 - v_{Al_xGa_{1-x}As}}{1 + v_{Al_xGa_{1-x}As}} + a^{\parallel}_{GaAs}\frac{2v_{Al_xGa_{1-x}As}}{1 + v_{Al_xGa_{1-x}As}}, \tag{2}$$

where $v_{Al_xGa_{1-x}As} = xv_{AlAs} + (1-x)v_{GaAs}$, and relation (2) can be written as

$$a^{v}_{Al_xGa_{1-x}As} = a^{\perp}_{Al_xGa_{1-x}As}\frac{1-(xv_{AlAs} + (1-x)v_{GaAs})}{1+(xv_{AlAs} + (1-x)v_{GaAs})} + a^{v}_{GaAs}\frac{2(xv_{AlAs} + (1-x)v_{GaAs})}{1+(xv_{AlAs} + (1-x)v_{GaAs})}. \tag{3}$$

Figure 2a shows the X-ray diffraction profile for the AlGaAs/GaAs(100) epitaxial heterostructure (sample EM1017). The alloy of this heterostructure was grown by MOCVD under standard conditions. We can see that diffraction from the (600) plane is an overlap of two $K\alpha_{1,2}$ doublets: the first one shifted to small angles is related to the AlGaAs alloy, the second doublet is caused by the single-crystal GaAs (100) substrate. The diffraction profiles were resolved into components using the SigmaPlot 10 software package, which makes it possible to minimize resolution errors to automatic simulating profile selection. The experimental diffraction profile was simulated beginning with resolution of the $K\alpha_{1,2}$ doublet of the GaAs (100) substrate. To this end, the GaAs (100) substrate's doublet was subtracted from the total profile, taking into account that the epitaxial film slightly weakens the Bragg reflection from the substrate due to its small thickness, ~1 μm, since the X-ray's half-value layer of the system under study is ~17 μm. Then, alloy diffraction was separated from the obtained diffraction curve. Based on the data obtained, the half-width of diffraction $K\alpha_{1,2}$ doublets was determined and the interplane distances were calculated. The alloy lattice's parameter was calculated according to expressions (1)–(3) taking into account internal strains, and the Poisson ratios used in calculations were taken from the published data, $v_{AlAs} = 0.255$ [8, 9] and $v_{GaAs} = 0.312$ [10]. The data obtained according to the above technique allow us to conclude that the lattice parameter, taking into account internal strains for the AlGaAs alloy (sample EM1017), satisfies the Vegard's law for the AlAs–GaAs system [7].

The (600) diffraction profiles of epitaxial heterostructures EM1540, EM1555, and EM1585, shown in Figs. 2b–2d were resolved into composing $K\alpha_{1,2}$ doublets in a similar way. For sample EM1540 which is a homoepitaxial GaAs/GaAs (100) heterostructure, the $K\alpha_{1,2}$ doublet of the film exactly coincides with the doublet of the substrate. At the same time, the half-width of the total diffraction profile of heterostructure EM1540 remains unchanged in comparison with the GaAs (100) single-crystal wafer used as a substrate

Table 2. Results of X-ray diffraction analysis and X-ray microanalysis of AlGaAs/GaAs (100) heterostructures

Heterostructure		Half-width, $\Delta\theta^\circ$	a_{exp}, Å	Composition x	a^V, Å
EM1017	$Al_xGa_{1-x}As$	0.08	5.6604(6)	0.510	5.6572
	GaAs (100)	0.08	5.6532(0)		5.6532
EM1540	$Al_xGa_{1-x}As$	0.06	5.6532(6)	0	5.6532(6)
	GaAs (100)	0.06	5.6532(6)		5.6532
EM1555	$Al_xGa_{1-x}As$	0.11	5.6461(2)	0.478	5.6492(8)
	GaAs (100)	0.07	5.6532(0)		5.6532
EM1585	$Al_xGa_{1-x}As$	0.18	5.6321(4)	0.4384	5.6415(6)
	GaAs (100)	0.06	5.6532(0)		5.6532

during the structure growth, which indicates the dislocation-free mechanism of such growth and excellent matching of film and substrate lattices.

As seen in Figs. 2c and 2d, diffraction of samples EM1555 and EM1585 is also an overlap of doublets of the GaAs (100) substrate and AlGaAs alloy. However, in contrast to heterostructure EM1017 grown by the standard technique, the arrangement of $K\alpha_{1,2}$ doublets of the film and substrate for low-temperature heterostructures differs significantly. The $K\alpha_{1,2}$ doublet of the AlGaAs epitaxial alloy is positioned on the side of large angles 2θ of the GaAs (100) doublet. This results from the fact that the AlGaAs lattice parameter is smaller than the GaAs (100) parameter.

The lattice parameters were calculated taking into account internal strains for low-temperature epitaxial heterostructures and assuming that the Poisson ratios for binary GaAs and AlAs compounds, determined by the new technique, are identical to the ratios given in [8–10]. The calculated parameters are listed in Table 1. An analysis of the data obtained allows the conclusion that the lattice parameters of the AlGaAs alloy obtained at lower temperatures are not identical to the lattice parameters of unordered alloys of the same compositions, proceeding from the Vegard's law for the AlAs–GaAs system [7]. However, noteworthy is that the lattice parameter of the low-temperature epitaxial alloy increases with the Al concentration.

3.2. Electron Microscopy

The study of electron microscopy of the surface morphology of heterostructures grown by the new technology and under normal conditions yielded information on the surface quality of epitaxial films. Moreover, X-ray microanalysis helped to refine element contents in low-temperature alloys, since X-ray diffraction studies showed unexpected results. The refined contents listed in Table 2 were used in calculating the lattice parameters taking into account internal strains. It is also important that the gallium content in surface layers of low-temperature films, taking into account the measurement error, greatly exceeds that which should be inherent to compositions of unordered alloys. As for the surface morphology, as seen in Fig. 3b, the low-temperature alloy of heterostructure EM1585 has an almost smooth surface in contrast to the surface of the alloy of standard sample EM1017, which contains slight imperfections (Fig. 3a).

3.3. IR Reflectance Spectra

Taking into account that growth of low-temperature epitaxial AlGaAs alloy with changed lattice

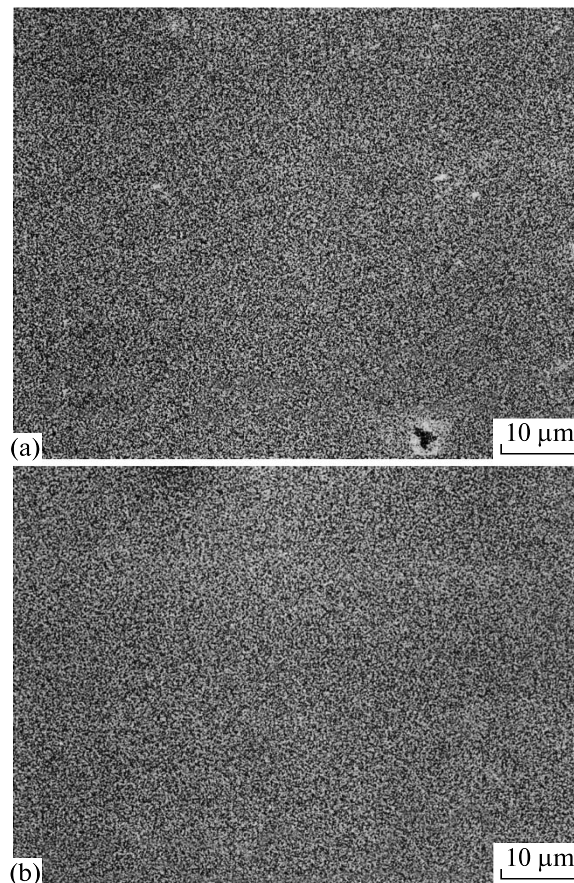

Fig. 3. SEM images of surface areas of epitaxial heterostructures (a) EM1017 and (b) EM1585.

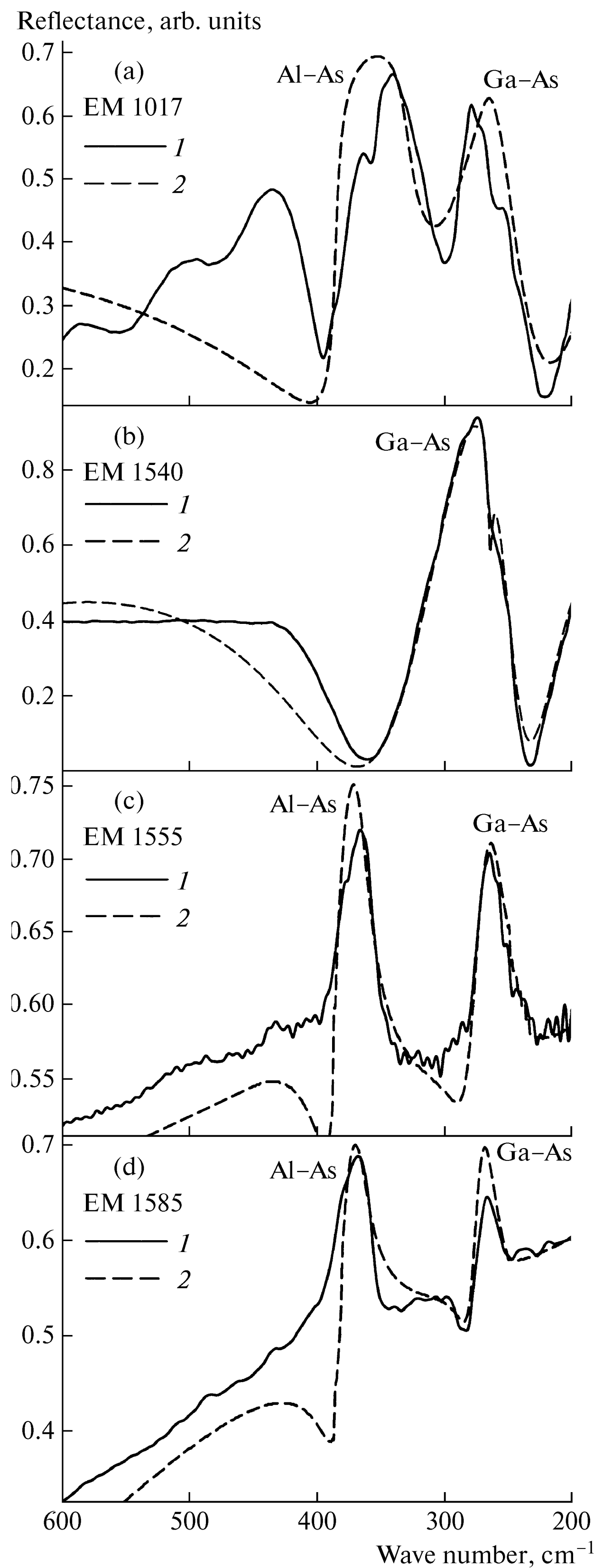

Fig. 4. IR reflectance spectra of AlGaAs/GaAs (100) heterostructures (a) EM1017, (b) EM1540, (c) EM1555, and (d) EM1585: (*1*) experiment and (*2*) model.

parameters in comparison with unordered alloys should also inevitably appear in optical spectra. We studied IR reflectance spectra of these heterostructures in the one-phonon resonance region.

Due to high penetrability of IR radiation, IR reflectance spectra of lattice vibrations make it possible to obtain information on the actual state of the crystal microstructure at a significant thickness, in order to estimate fine lattice properties and internal strains to which this method is very sensitive. The experiment shows that the reflectance spectra of unordered AlGaAs alloys of different compositions ($0 < x < 1$) always contain two fundamental vibrational modes, which corresponds to the criterion of estimation of the transformation type of the vibrational spectrum [11], which specifies a two-mode transformation type for vibrational spectra of the AlGaAs alloy. These are fundamental vibrations to which the Al–As mode (the intensity of this mode increases with the Al content in the AlGaAs alloy) and the Ga–As mode (antibatically changing its intensity with respect to the Al–As mode, i.e., according to the Ga content in the AlGaAs alloy) are attributed.

Experimental data are also confirmed by calculations of TO and LO modes of IR reflectance spectra of AlGaAs alloys for different x, performed within the modified model of statistical isovalent substitution in mixed crystalline systems (MREI model [12]) with a specified type of vibrational spectrum transformation. The data on LO and TO frequencies of vibrations, obtained in [12] are in good agreement with the experimental results of [13]. Moreover, the studies [12, 13] clearly demonstrate variation in the TO and LO vibrational mode's positions on the frequency scale with the Al content in the AlGaAs alloy.

IR reflectance spectra of epitaxial heterostructures were simulated in the models of a semi-infinite substrate and a surface thin film of thickness d with dielectric functions ε_s and ε_f, respectively. In this model, the normal-incidence reflectance is written as [11]

$$R = \left|\frac{r_f(\omega) + r_{fs}(\omega)\exp(i2\beta)}{1 + r_f(\omega)r_{fs}(\omega)\exp(i2\beta)}\right|^2, \quad (4)$$

where

$$r_f(\omega) = \frac{1-\sqrt{\varepsilon_f(\omega)}}{1+\sqrt{\varepsilon_f(\omega)}}, \quad r_{fs} = \frac{\sqrt{\varepsilon_f(\omega)} - \sqrt{\varepsilon_s(\omega)}}{\sqrt{\varepsilon_f(\omega)} + \sqrt{\varepsilon_s(\omega)}},$$
$$\beta = \frac{2\pi d\sqrt{\varepsilon_f(\omega)}}{\lambda}, \quad (5)$$

and $\lambda = 10000/\omega$ is the wavelength.

The film's dielectric function was set taking into account the adiabatic approximation

$$\varepsilon_f(\omega) = \varepsilon_\infty + \sum_i \frac{4\pi f_i(\omega_{\mathrm{TO}i})^2}{(\omega_{\mathrm{TO}i})^2 - \omega^2 + i\omega\gamma_i}, \quad (6)$$

where f_i, ω_i, and γ_i are the strength, resonant frequency, and damping of the ith oscillator.

For example, Fig. 4a shows the experimental and calculated IR reflectance spectra of the AlGaAs/GaAs (100) epitaxial heterostructure with $x \approx 0.50$ (sample EM1017). We can see that the spectrum contains two fundamental vibrational modes whose frequencies of TO and LO modes are identical to those given in [12, 13]. The increase in the reflectance in the range of 400–500 cm^{-1} is caused by the onset of plasma oscillations occurring due to GaAs (100) substrate doping.

The IR reflectance spectrum of the homoepitaxial low-temperature heterostructure EM1540 is shown in Fig. 4b. We can see from epitaxial and calculated data that the spectrum contains a single phonon mode in the range of 250–350 cm^{-1}. The appearance of the plasmon–phonon resonance in the band of 300–350 cm^{-1}, as in the case of sample EM1017, has an effect on the reflectance spectrum.

The spectra of low-temperature epitaxial heterostructures of samples EM1555 and EM1585 (Figs. 4c, 4d), as the spectrum of sample EM1017, contain two fundamental phonon modes Al–As and Ga–As. However, as dispersion analysis showed, first, the fundamental modes of these vibrations are not identical to modes of unordered alloys of similar compositions neither in frequencies nor in intensities of TO and LO phonons (which are extraordinarily small) [12, 13]. Moreover, the dependence of frequency of longitudinal and transverse modes of fundamental vibrations on the atomic concentration in the metal sublattice is not identical to the same dependences obtained in [12, 13]. Second, simulation showed that the high-frequency permittivity ε_∞ of low-temperature films is extraordinarily high and is almost twice the high-frequency permittivity ε_∞ of the alloy of the conventional heterostructure. Noteworthy is also the extraordinarily smooth slope of the reflectance in the far IR region for low-temperature epitaxial heterostructures, which is more likely characteristic of metals, rather than semiconductors. Significant differences between experimental spectra of low-temperature heterostructures and those calculated in the film–substrate model are observed only in the reflectance slope's region.

4. CONCLUSIONS

The analysis of the data obtained by X-ray diffraction, scanning electron microscopy, and IR spectroscopy allows several important conclusions on the structure of AlGaAs alloys grown by new technology.

Epitaxial films of low-temperature AlGaAs alloys, as well as unordered solid solutions, are characterized by the sphalerite structure, which is well enough traced in the case of GaAs/GaAs(100) homoepitaxial structure growth, since, as follows from the X-ray diffraction results, the alloy and substrate lattices are perfectly matched. However, a significant difference is that the lattice parameter of the epitaxial film grown at a lower temperature is smaller than that of GaAs, although it increases with the Al content in the metal sublattice, which contradicts the generally known Vegard's law [7]. These data obtained initially by analyzing the results of X-ray diffraction are also confirmed by IR spectroscopy, proceeding from the data on frequencies and intensities of TO and LO phonons of fundamental modes. It should also be noted that the composition of low-temperature alloys, calculated from the data determined for layers growing under normal conditions (the growth temperature is 600–700°C and the ratio of Group-V and -III elements is ~100–200) is not identical to that determined by X-ray microanalysis.

A similar study of the structural quality of AlGaAs films was performed in [14, 15], where samples based on AlGaAs alloys were prepared by molecular-beam epitaxy (MBE) at low temperatures (~250°C). However, as shown in [14, 15], an excess of arsenic atoms in films was observed during low-temperature MBE, which could form clusters orderly arranged in the film bulk; therefore, the lattice parameter of low-temperature AlGaAs was larger than that of normal solid solutions. Subsequent annealing of films redistributed excess arsenic and resulted in a decrease in lattice parameters to values "normal" for given contents.

However, to explain the fact that growth of hydride-MOCVD AlGaAs alloys at a lower temperature and a minimum ratio of Group-V and -III elements are accompanied by a decrease in the lattice parameter, we had to assume that gallium atoms in the metal sublattice are not substituted with aluminum atoms, and freed sites remain vacant. However, to this end, vacancies should be formed only at the centers of sphalerite lattice faces, since the alloy's lattice parameter can be smaller than that of GaAs only under such condition. Several established facts argue in favor of this assumption. First, as was shown by X-ray microanalysis, a small excess of gallium atoms is observed in surface layers of low-temperature films, which probably left the metal sublattice, but were not substituted with aluminum. Therefore, IR reflection from such films changed in comparison with spectra of unordered alloys, which is also confirmed by calculations in the film–substrate model. Second, the results of X-ray diffraction show that half-widths of (600) diffraction line of low-temperature alloys are appreciably larger than those of the alloy grown by the conventional technology; and as is known, changes in diffraction line half-widths can indicate structure imperfection, i.e., vacancy formation in the lattice.

Thus, based on the results obtained, it can be argued that thermodynamic conditions of epitaxial growth at a lower temperature and a minimum ratio of Group-V and -III elements result in that the AlGaAs omission's solid solution is formed at aluminum atom contents $0 < x < 1$.

However, the formation of the $AlGaAs_2$ chemical compound with the parameter smaller than that of GaAs during the formation of superstructure phases [1–3] was caused by kinetic transformations of the solid solution, i.e., its separation into phases due to internal lattice strains, which resulted in layer ordering of Al and Ga arrangement in the III sublattice and tetragonal compression along the lattice growth axis; whereas, in the case of epitaxial growth by the low-temperature technology, the structure transformation with the formation of omission solid solutions is caused by thermodynamic-type instability with respect to spontaneous separation into phases, and the elastic energy actuating this mechanism arises most likely due to the requirement for coherent (dislocation-free) conjugation of separated phases.

The authors propose to continue the study of this heterostructure type; in particular, the problem of the parameters of bandgaps of these samples remains open.

ACKNOWLEDGMENTS

The authors are grateful to E.I. Zavalishin and A.N. Lukin (department of Solid State Physics and Nanostructures) for helpful suggestions in discussing the results of the study.

This study was supported by the Russian Foundation for Basic Research.

REFERENCES

1. É. P. Domashevskaya, N. N. Gordienko, N. A. Rumyantseva, P. V. Seredin, B. L. Agapov, L. A. Bityutskaya, I. N. Arsent'ev, L. S. Vavilova, and I. S. Tarasov, Fiz. Tekh. Poluprovodn. **42**, 9 (2008) [Semiconductors **42**, 1069 (2008)].
2. É. P. Domashevskaya, P. V. Seredin, É. A. Dolgopolova, I. E. Zanin, I. N. Arsent'ev, D. A. Vinokurov, A. L. Stankevich, and I. S. Tarasov, Fiz. Tekh. Poluprovodn. **39**, 3 (2005) [Semiconductors **39**, 336 (2005)].
3. E. P. Domashevskaya, P. V. Seredin, A. N. Lukin, L. A. Bityutskaya, M. V. Grechkina, I. N. Arsent'ev, D. A. Vinokurov, and I. S. Tarasov, Surf. Interf. Analysis **8**, 828 (2006).
4. A. Zunger, MRS-IRS Bulletin/July 1997; http://www.sst.nrel.gov/images/mrs97.
5. W. B. Pearson, *Crystal Chemistry and Physics of Metals and Alloys* (New York, Wiley, 1972).
6. V. S. Zemskov, *Solid Solutions in Semiconductor Systems*, the Handbook (Nauka, Moscow, 1978) [in Russian].
7. Yu. A. Goldberg, in *Handbook Series on Semiconductor Parameters*, Ed. by M. Levinshtein, S. Rumyantsev, and M. Shur (World Sci., London, 1999), v. 2. p. 1.
8. D. Zhou and B. F. Usher, J. Phys. D: Appl. Phys. **34**, 1461 (2001).
9. Z. R. Wasilewski, M. M. Dion, D. J. Lockwood, P. Poole, R. W. Streater, and A. J. Spring Thorpe, J. Appl. Phys. **81**, 1683 (1997).
10. S. Adachi, J. Appl. Phys. **58**, R1 (1985).
11. L. K. Vodop'yanov, S. P. Kozyrev, and Yu. G. Sadof'ev, Fiz. Tverd. Tela **41**, 982 (1999) [Phys. Solid State **41**, 893 (1999)].
12. I. F. Chang and S. S. Mitra, Phys. Rev. B **2**, 1215 (1970).
13. M. Ilegems and G. L. Pearson, Phys. Rev. B **1**, 1576 (1970).
14. S. Fleisher, C. D. Beling, S. Fung, W. R. Nieveen, J. E. Squire, J. Q. Zheng, and M. Missous, J. Appl. Phys. **81**, 190 (1997).
15. A. V. Boitsov, N. A. Bert, V. V. Chaldyshev, V. V. Preobrazhenskii, M. A. Putyato, and B. R. Semyagin, Fiz. Tekh. Poluprovodn. **43**, 278 (2009) [Semiconductors **43**, 266 (2009)].

Translated by A. Kazantsev